X-ray study of the modulated structure in as-grown Ga$_2$Te$_3$ crystals with the defect zinc-blende lattice

Y. Otaki [1], Y. Yanadori [2], Y. Seki [3], M. Tadano, S. Kashida *

Graduate School of Science and Technology, Niigata University, Ikarashi 8050, Niigata 950-2181, Japan

A B S T R A C T

Ga$_2$Te$_3$ crystallizes in the zinc-blende structure, where one third of the cation sites are vacant. Single crystal X-ray diffraction studies were done on as-grown Ga$_2$Te$_3$ crystals. The diffraction measurements show, other than the zinc-blende type main reflections, satellite reflections at $q \approx 1/20(210)_c$, where the subscript c means the cubic sub-lattice. The analysis of the satellite reflections shows that the crystal contains a two-dimensional modulation with $q_1 \approx 1/20(210)_c$ and $q_{1'} \approx 1/20(2\bar{1}0)_c$. The modulated structure is composed of a coupled mode of the amplitude type modulation caused by Ga vacancies and the accompanying displacive modulation of surrounding Te atoms, which has the polarization vector along the $[001]_c$ direction. The nature of the atomic modulations is argued and the origin of the modulation is ascribed to the local distortion around a Ga vacancy.

© 2009 Elsevier Inc. All rights reserved.

1. Introduction

Metal sesqui-chalcogenides, $M_2^{III} X_3^{VI}$ (where $M =$ Ga, or In and $X =$ S, Se or Te) crystallize in the zinc-blende or wurtzite structure, where one-third of the cation sites is vacant in order to satisfy the chemical valencies. These vacancies noted as "structural vacancies" are inevitable to hold tetrahedral crystal structures. The orderings of the large amount of vacancies have received crystallo-chemical interest, and have been studied for a fairly long time. In earlier works on Ga$_2$S$_3$, Ga$_2$Se$_3$ and Ga$_2$Te$_3$, Hahn and Klinger [1] reported that Ga$_2$S$_3$ crystallizes in zinc-blende and wurtzite structures and that Ga$_2$Se$_3$ and Ga$_2$Te$_3$ crystallize only in the zinc-blende structure. The authors observed only main reflections and concluded that the crystals contain random distributions of cation vacancies. In subsequent works [2,3], it was recognized that, by annealing, Ga$_2$S$_3$ and In$_2$Se$_3$ crystallize into wurtzite based superlattice structures, while Ga$_2$Se$_3$ and Ga$_2$Te$_3$ crystallize into zinc-blende based superlattice structures. From powder X-ray diffractions, it was reported that Ga$_2$Te$_3$ has an orthorhombic structures with unit cells $a = 1/2[110]_c$, $b = 4[001]_c$ and $c = 3/2[1\bar{1}0]_c$ [2], and that Ga$_2$Se$_3$ has a monoclinic structure $a = 1/2[112]_c$, $b = 3/2[1\bar{1}0]_c$ and $c = 1/2[11\bar{2}]_c$ [3], where the subscript c means the cubic zinc-blende lattice.

In recent electron diffraction and electron microscopic studies done on Ga$_2$Te$_3$, by Hanada et al. [4] and Kienle et al. [5], observed satellite reflections at $1/10[111]_c$. These authors attributed the satellites to gatherings of the structural vacancies at every ten layer along the [111] axis. Hanada et al. [4] also reported that if the ordering of structural vacancies occurs at four $\langle 111 \rangle_c$ directions, equivalently, the total amount of vacancies becomes the nominal value 1/3; the vacancy ordering along a $\langle 111 \rangle_c$ direction causes 1/10 of the cation sites vacant, the ordering along another $\langle 111 \rangle_c$ direction causes 1/10 of the filled cation sites, $(1-1/10) \times 1/10$, further vacant. Therefore, the total amount of vacancies becomes $1/10 + (1 - 1/10) \times 1/10 + (1 - 1/10)^2 \times 1/10 + \cdots = 0.34$.

In order to investigate the nature of the vacancy orderings, we have been performing single crystal X-ray diffraction studies of Ga$_2$Te$_3$. In a recent study, we found that quenched Ga$_2$Te$_3$ crystals show satellites at $q \approx (0.06\,0.06\,0.0)_c$ [6]. In defect zinc-blende compounds, it is well known that the ordering of vacancies depends upon its thermal history. In this paper, we report on X-ray diffraction study of as-grown Ga$_2$Te$_3$ crystals.

* Corresponding author. Fax: +81 25 262 6131.
E-mail address: kashida@sc.niigata-u.ac.jp (S. Kashida).
[1] Present address: Citizen Electronics Co. Ltd., Kamikurechi, Fujiyoshida, Yamanashi 403-0001, Japan.
[2] Present address: Nagaoka City Office, 2-4-9 Ote Street, Nagaoka, Niigata 940-0062, Japan.
[3] Present address: Nippon Light Metal Co. Ltd., 161 Kambara, Shimizu-ku, Shizuoka 421-3297, Japan.
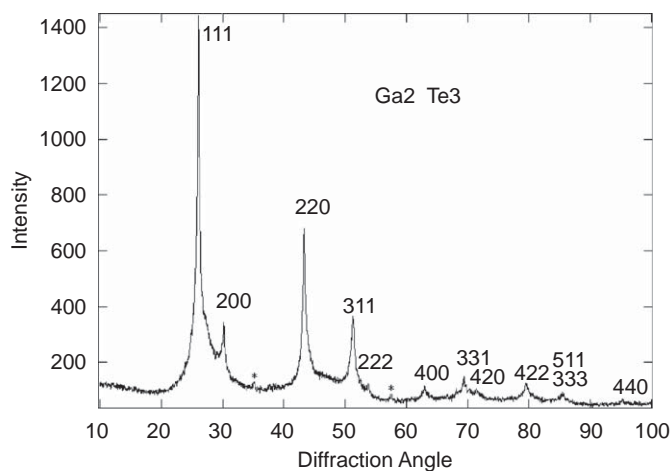
2. Experimentals

Single crystal samples of Ga_2Te_3 were grown by direct reaction of the elements. A mixture containing appropriate amounts of Ga and Te (99.999%), was sealed in an evacuated quartz ampoule and set in a furnace. The temperature of the furnace was raised above the melting temperature of Ga_2Te_3 (1065 K) held at 1133 K for 12 h, and was decreased at the rate of 6 K/h down to 853 K. Then the furnace was shut off and the sample was allowed to cool to room temperature over about three hours. The obtained samples were aggregations of small crystals. The crystals have metallic luster with most surfaces terminated by $\langle 111 \rangle_c$ planes.

Preliminary studies were done by taking powder X-ray scattering patterns and Buerger precession photographs in order to survey the diffraction pattern and check the crystal symmetry. The intensity data were collected by step scanning in reciprocal space using a Huber four-circle diffractometer with graphite monochromated $MoK\alpha$ radiation. The resolution of the diffract-ometer is, about 0.06 (full width at half maximum, FWHM) in the longitudinal direction (toward the reciprocal origin), and about 0.02 (FWHM) in the transversal direction (both in unit of a^*, where we used the cubic lattice parameter of Ga_2Te_3, $a_0 = 5.895(5)$). Details of the used diffractometer are reported elsewhere [6].
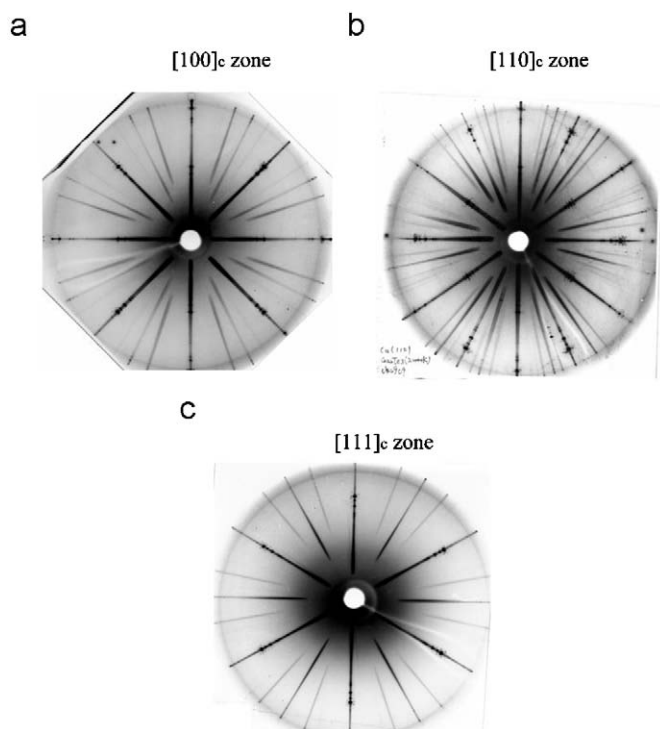
3. Experimental results and discussion

3.1. General aspect of the diffraction pattern of as-grown Ga_2Te_3 crystals

The powder diffraction pattern of as-grown Ga_2Te_3 crystals, taken with graphite monochromated $CuK\alpha$ radiation is shown in Fig. 1. The diffraction peaks can be indexed by the cubic zinc-blende lattice with $a_0 \approx 5.9$ Å. However, a close inspection of the data reveals the following two points. Firstly, small extra peaks are observed at 35° and 57° (denoted by asterisks in Fig. 1). Comparing the diffraction pattern with that of $CuGaTe_2$, these peaks are indexed as (211/2) and (321/2), corresponding to chalcopyrite structure which has the unit cell $a = b = a_0$ and $c = 2a_0$. These extra peaks are absent in quenched Ga_2Te_3 crystals, indicating the existence of chalcopyrite type orderings in

Fig. 2. (a) Precession photographs of as-grown Ga_2Te_3 crystals, taken with Cu radiation. (a) The $[100]_c$ zone, horizontal: $[010]_c$ axis, and vertical: $[001]_c$ axis. (b) The $[110]_c$ zone, horizontal: $[1\bar{1}0]_c$ axis, and vertical: $[001]_c$ axis. (c) The $[111]_c$ zone, horizontal: $[11\bar{2}]_c$ axis, and vertical $[1\bar{1}0]_c$ axis.
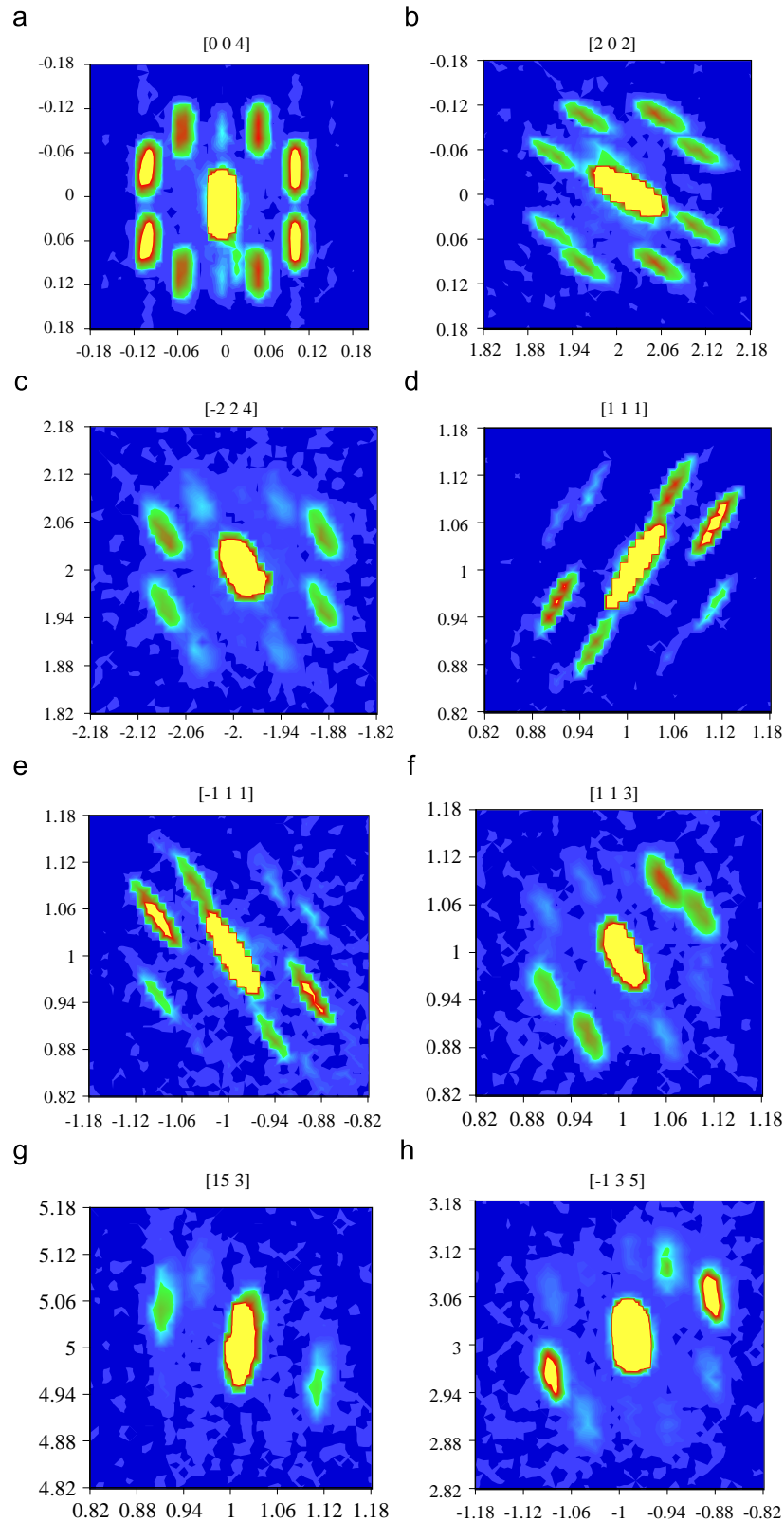
as-grown Ga_2Te_3 crystals. Secondly, the width of the Bragg diffrac-tion peak is abnormally wide, suggesting that the crystals contain large local strains. These points will be argued again in a later section. The precession photographs taken with Cu radiation are shown in Figs. 2(a)–(c). These photographs indicate main Bragg reflections ascribable to the cubic zinc-blende structure. Fig. 2(b) also reveals weak diffuse streaks along the $\langle 111 \rangle_c$ direction. The diffuse streaks have a broad maximum around $q \approx 1/2(111)_c$ indicating an anti-ferro type short range ordering of vacancies along the $\langle 111 \rangle_c$ direction. The result will be compare with those of recent electron diffraction studies of annealed Ga_2Te_3 crystals [4,5], where satellite reflections are observed at $1/10[111]_c$.

A close inspection of the precession photographs also disclosed fine satellite reflections around the main reflections, which are not resolved well in Figs. 2(a)–(c). In order to search for the satellite positions, detailed diffraction measurements were done step by step in the reciprocal space at points with spacing 0.01 along the a^* and b^* axes and 0.025 along the c^* axis. Figs. 3(a)–(k) show X-ray intensity maps of as-grown Ga_2Te_3 crystals taken around several main reflections. For comparison, the contour map taken in quenched Ga_2Te_3 crystal is shown in Fig. 3(l).

3.2. Analysis of the satellite diffraction

The contour maps show the followings.

(i) The satellite reflections appear at $q \approx (0.089(9)\ 0.050(7)\ 0.000(6))_c$ and equivalent positions, where the figure in the parentheses shows the standard deviation estimated using the positions of several equivalent satellite reflections. This shows that the as-grown Ga_2Te_3 crystals have a long period incommensurate structure, the modulation wave vector is

Fig. 1. Powder diffraction pattern of as-grown Ga_2Te_3 taken with $CuK\alpha$ radiation. The diffraction pattern is indexed using the cubic zinc-blende lattice. The small peaks at 35° and 57°, marked by asterisks, are indexed as (211/2) and (321/2). These reflections correspond to the chalcopyrite ($CuFeS_2$) type structure.

Fig. 3. (a)–(k). Contour maps of as-grown Ga_2Te_3 crystal, taken in the a^*(horizontal)–b^*(vertical) plane around several main Bragg reflections, where contours are drawn in linear but arbitrary scale. Contour maps of as-grown Ga_2Te_3 crystals taken around the (004) main Bragg reflection, the same as Fig. 3(a), but in a wider region. Note in Figs. 3(a) and (k) that strong satellite reflections are observed $q_1 = (0.089\,0.050\,0.00)_c$ and $q_{1'} = (0.089\,-0.050\,0.00)_c$ (denoted by a in Fig. 3(k)). The faint diffractions at $q_2 = (0.18\,0.10\,0.00)_c$ and equivalent positions (denoted by b) are the second order satellites. Also the faint diffractions at $q_{2'} = (0.00\,0.10\,0.00)_c$ and $q_{2''} = (0.18\,0.00\,0.00)_c$ (denoted by c) are the second order satellites derived from $q_1-q_{1'}$ and $q_1+q_{1'}$. The satellites at $q_3 = (0.050\,0.089\,0.00)_c$ and $q_{3'} = (-0.050\,0.089\,0.00)_c$ are due to twins. Note also that the satellites at $q_1 = (0.089\,0.050\,0.00)_c$ and $q_{1'} = (0.089\,-0.050\,0.00)_c$ have equal intensity in 3(a)–(c), but the satellite at $q_1 = (0.089\,0.050\,0.00)_c$ is stronger in 3(d), (f), (h) and (i), while the satellites are at $q_{1'} = (0.089\,-0.050\,0.00)_c$ is stronger at 3(e), (g) and (j), (see, text). (l) Contour maps of quenched Ga_2Te_3 crystal, taken in the a^*(horizontal)–b^*(vertical) plane around the (004) main Bragg reflection.
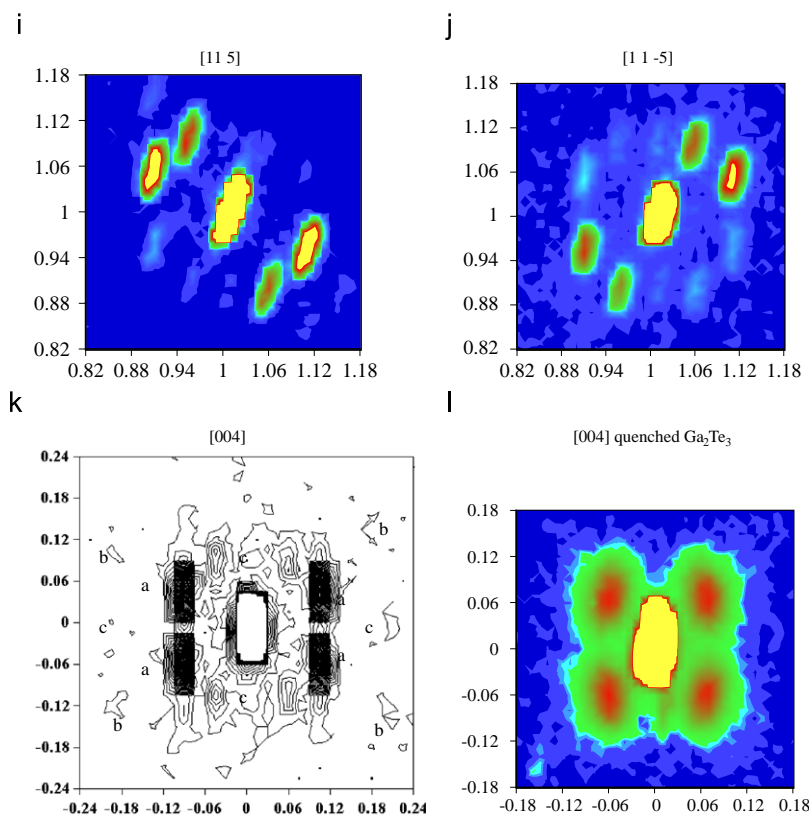
Fig. 3. (*Continued*)

nearly parallel to the $[210]_c$ direction, $q \approx 1/20(210)_c$. The results are in contrast to previous electron diffraction results on annealed crystals [4,5], where the satellite reflections are observed at $q \approx 1/10(111)_c$, it is also in contrast with those of quenched crystals where the satellites are observed at $q \approx 1/17(110)_c$ [6].

(ii) The relative intensity of the satellite to the main Bragg reflection, which has the indices (*hkl*), increases as the index *l* increases, see Fig. 4.

(iii) The satellite reflections indicate the following peculiar intensity rules.

   (a) Firstly, around the $(00l)_c$ main reflection, satellite reflections appear at transverse planes normal to the direction from $O = (000)$ to $(00l)_c$, but do not appear at longitudinal planes which include the direction from $O = (000)$ to $(00l)_c$.

   (b) Secondly, in the a^*–b^*-plane if the indices of the main reflection are even, the satellites appear at $q \approx 1/20(210)_c$ and $q \approx 1/20(2\bar{1}0)_c$ with almost equal intensity (see, Figs. 3(a)–(c)), however, if the indices of the main reflection are odd, the intensity is not equal; if $h+k+l = 4n-1$, the satellite at $q \approx 1/20(210)_c$ is stronger, while if $h+k+l = 4n+1$, the satellite at $q \approx 1/20(2\bar{1}0)_c$ is stronger (see, Figs. 3(d)–(f)). This inequality relation is reversed when the index *l* is changed to –*l* (cf. Figs. 3(g) and (h)).

(iv) An asymmetry of the intensity exists between a pair of satellites centered about the main Bragg reflection; the intensity of the higher angle satellite is stronger than that of the lower angle counterpart, see Figs. 3(d) and (g).

(ii) and (iii-a) indicate that the modulation is of transverse displacement type; the modulation wave vector is nearly parallel to $[210]_c$, while the direction of displacements is nearly parallel to $[001]_c$. For the analysis of the observed intensity rule (iii-b), we calculate the structure factor in the appendix, where both the amplitude and displacive modulations are taken into account. When we assume that the magnitude of the amplitude modulation caused by Ga vacancies and that of the displacive modulation of the surrounding Te atoms are comparable and also in phase, the calculated structure factor A(7) reproduces the observed intensity rule, i.e., for the satellite reflections with $q \approx 1/20(210)_c$, if the main reflection has odd indices with $h+k+l = 4n-1$ the first order satellite reflection appears, but, if $h+k+l = 4n+1$ the satellite reflection disappears. The present diffraction data show also that, for the satellite reflections with $q \approx 1/20(2\bar{1}0)_c$ the reverse is true. These facts indicate that the modulation waves traveling along the $[210]_c$ and $[2\bar{1}0]_c$ directions are out of phase (see, Fig. 5). It should be noticed that the present incommensurate structure is two dimensional and the satellite reflections with $q \approx 1/20(210)_c$ and $q \approx 1/20(2\bar{1}0)_c$ are inseparable. It will be compared with previous electron diffraction data of annealed crystals where a one-dimensional ordering of the vacancies was found along the $\langle 111 \rangle_c$ axis [4,5]. From the appearance of the satellite reflections, the present structure is classified to the super-space symmetry $Fmmm(\alpha\beta0)$, with the face centered orthorhombic cell $a_0 = [100]_c$, $b_0 = [010]_c$ and $c_0 = [001]_c$, which is equivalent to $Fmmm(0\beta\gamma)$ in Ref. [7].

3.3. Analysis of the deformation waves

As to the origin of the displacement wave, several mechanisms will be considered, such as the atomic size effect and the Jahn–Teller effect which is caused by the degeneracy of the dangling orbitals around a cation vacancy [8,9]. A detailed
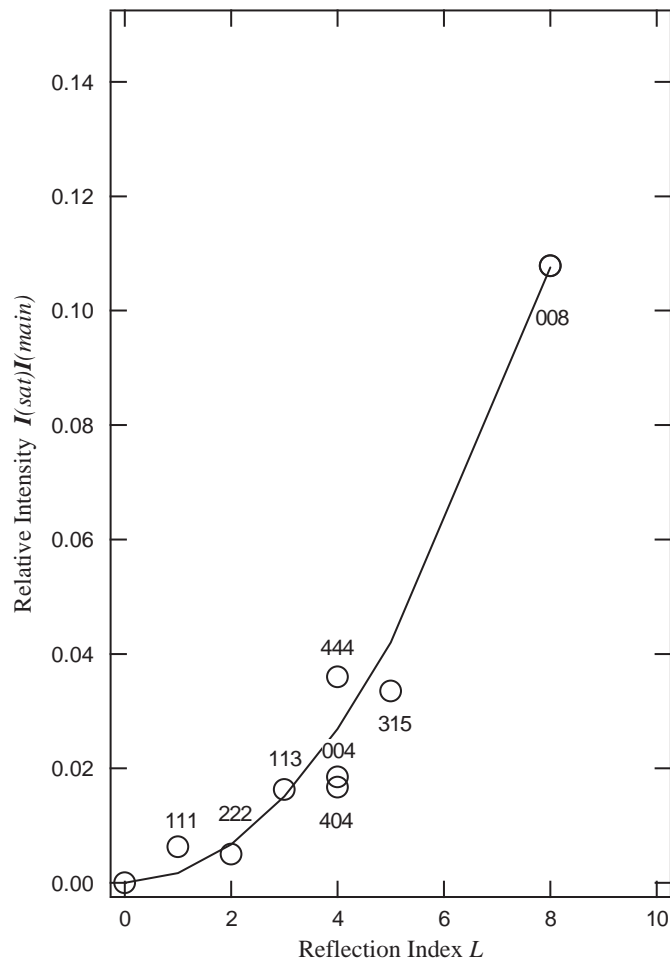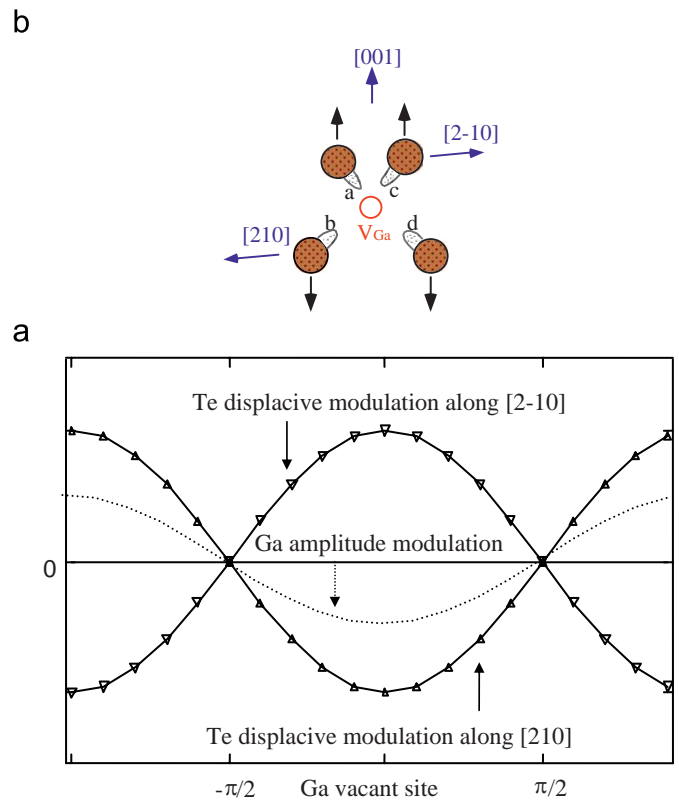
Fig. 4. Relative intensity of the satellite reflections taken in as-grown Ga_2Te_3 crystal plotted as a function of the index l of the main Bragg reflections. The (hkl) indices of the used main reflections are indicated and the curve shows l^2 dependence of the relative intensity.

Fig. 5. (a) Schematic drawing of the modulations observed in as-grown Ga_2Te_3. Note that the displacement wave of Te atoms traveling along the $[2\bar{1}0]_c$ direction is in anti-phase with that traveling along the $[210]_c$ axis. (b) Tetragonal local distortion around a Ga vacancy, derived from the phase relations shown in Fig. 5(a).

analysis of the vacancy-induced atomic relaxation was performed by Bernard and Zunger [10]. Comparing the phase relations among the amplitude modulation and the displacement modulations traveling along the $[210]_c$ and $[2\bar{1}0]_c$ directions shown in Fig. 5, we think that the tetragonal distortion around a Ga vacancy (Fig. 5(b)) is the motif of the modulated structure. The results of the previous electron diffraction [4,5] and the present X-ray diffraction suggest that the defect zinc-blende compound Ga_2Te_3 has a tendency to dissociate periodically into Ga rich and Ga poor regions.

The thermodynamics of decomposition in solid-solutions have been studied by Khachaturyan [11]. It is known that the direction of compositional modulation is determined so as to minimize the elastic energy [12]. The modulation wave will be parallel to the "soft direction", in this case, to the [001] direction, since the condition $C_{44} > 1/2(C_{11} - C_{12})$ is fulfilled in cubic tetrahedral semiconductors. In the present Ga_2Te_3 crystals, however, the direction of the modulation is $[210]_c$ in as-grown crystals, and $[110]_c$ in quenched crystals [6]. Considering that the structural modulation is derived from Ga vacancies, it will be evident that the propagation direction is dependent on atomic orderings.

In defect zinc-blende structure, Ga atom and Ga vacancy X form an fcc lattice, Ga_2X. The atomic orderings in fcc alloys have been studied thoroughly, where the $[210]_c$ type ordered structure is frequently observed in A_2B type alloys. Fig. 6 shows the structure of fcc alloys which are characterized by the $[210]_c$ type orderings, projected along the $[001]_c$ axis. We suppose that Ga_2Te_3

is unstable and dissociates into a Ga_3XTe_4 type structure in Ga rich region, and a chalcopyrite like $GaXTe_2$ type structure in Ga poor region. Both these two structures have the common $D0_{22}$ lattice. The above mentioned super-lattice reflections at $(211/2)$ and $(321/2)$ are derived from the $D0_{22}$ type atomic ordering. By annealing, Ga vacancies tend to occupy the third neighbor sites in the fcc lattice and gather in the $(210)_c$ plane, as shown in dotted lines in Fig. 6. In order to gain in the interaction energy between the local distortions, the phase of the modulation wave is adjusted so that they align in the vacant $(210)_c$ plane. Therefore, the propagation direction of the modulation wave will become normal to these aligned planes as indicated by arrows in Fig. 6.

The asymmetry of the satellite intensity (iv) is ascribed to the coupling between the amplitude modulation due to Ga vacancies and the displacement modulation of Te atoms. Around the Ga vacancy the electron density decreases, while due to the above distortion the lattice constant increases. If pairs of the atoms with large scattering factors have smaller lattice constants and pairs with smaller scattering factors have larger lattice constants, the satellite corresponding to the large angle is more intense than that at the lower angle [13]. It should be noticed that around the Ga vacancy the lattice constants increase. It is in contrast to the theoretical prediction that the chalcogen atoms would move toward the vacant sites [10]. We found that if as-grown crystals are annealed below the melting temperature for several weeks the satellites appear at $q \approx 1/10(111)_c$, as already reported in electron diffraction studies [4,5]. These facts indicate that the modulated structure in Ga_2Te_3 changes from $q \approx 1/17(110)_c$ in quenched crystals, through $q \approx 1/20(210)_c$ in as-grown crystals, and finally to $q \approx 1/10(111)_c$ in fully annealed crystals.

Ga2X   GaX+Ga3X
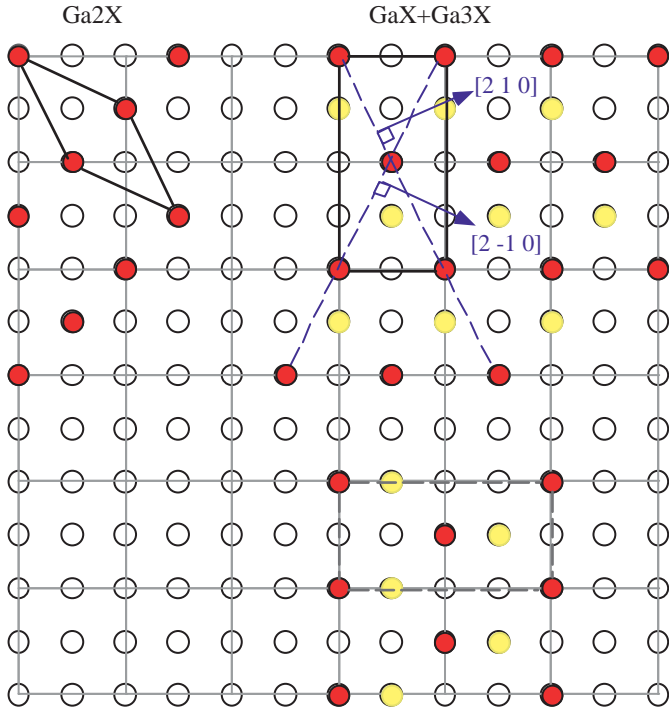
Fig. 6. The structure of AB type fcc alloy, projected along the $[001]_c$ axis. The left figure shows the monoclinic Ni_2Mo type structure, and the right upper figure shows the orthorhombic Ni_3Mo type ($D0_{22}$) structure. The $D0_{22}$ structure is closely related to the chalcopyrite structure, such as $CuGaSe_2$ and $CuGaTe_2$, and realized in In_3Te_4 [14]. The filled circles show the minor atoms (vacancies). If the sites expressed by half tone are occupied by vacancies the chalcopyrite like $GaXTe_2$ is obtained, and if these sites are fully occupied by Ga atoms the In_3Te_4 type Ga_3XTe_4 crystal is obtained. In the $D0_{22}$ structure, the minority atoms (vacancies) are arranged in the $(210)_c$ plane, as shown by the dotted lines, the direction of the modulation wave will be normal to these lines (see text). The right lower figure shows the arrangement of atoms in the twin variant, which yields satellites at $q_3 = (0.050\ 0.089\ 0.00)_c$ and $q_{3'} = (-0.050\ 0.089\ 0.00)_c$ in Figs. 3(a) and (k).

Lastly, we comment on the broadening of main Bragg reflections observed in powder diffractions (see, Fig. 1). Our single crystal contour maps show that the Bragg peaks have long trails along the $[210]_c$ direction, see, Figs. 3(b, d–g) and (i). The trail is most remarkable for low angle scatterings such as (111) and (202), for high angle scatterings, the trail is obscured by the tangential dispersion due to crystal mosaicness. The trail has the longitudinal component (toward the reciprocal origin), e.g., the (111) reflection has the trail along the $[120]_c$ direction (see, Fig. 3(d)), and gives rise to the line broadening observed in the powder diffraction pattern. We think that the broadening is caused by the collective distortion noted as, "Guinier–Preston zones" [13]. As mentioned above, Ga vacancies tend to gather in the $(210)_c$ plane. These precipitated planes have scattering power and lattice constant different from those of the surrounding matrix, and give rise to strong diffuse scattering normal to the plane causing elongated Bragg peaks along the $\langle 210 \rangle_c$ direction.

4. Conclusion

In this paper, we report on single crystal X-ray diffraction data of as-grown Ga_2Te_3 crystals. We found that the crystals show satellite reflections at $q \approx 1/20(210)_c$. From the analysis of the satellite reflections, the structure is ascribed to a coupled mode of the amplitude type modulation caused by Ga vacancies and the displacement modulation of surrounding Te atoms. The displacement modulation is traveling along the $[210]_c$ and $[2\bar{1}0]_c$ directions with the polarization vector along the $[001]_c$ direction. The nature of

the atomic modulations is argued, and the origin of the modulated structure is ascribed to the local distortion around a Ga vacancy. We are confident about having identified most prominent feature of the modulation. In order to determine the structure, however, full intensity data of the satellite reflections are needed.

Appendix A

In this appendix, the intensity of the satellite reflection is calculated. In the zinc-blende lattice, A (Ga) and B (Te) atoms occupy the sites (0,0,0) and (1/4,1/4,1/4), respectively. We take into account the amplitude modulation due to Ga vacancies and the displacive modulation of surrounding Te atoms,

$$\eta_{Ga} \sin\{2\pi(q_x na + q_y n'b) + \psi_{Ga}\} \tag{A.1}$$

and

$$w_{Te} \sin\{2\pi(q_x na + q_y n'b) + \chi_{Te}\} \tag{A.2}$$

where we take the modulation wave vector as $(q_x, q_y, 0)$, and η_{Ga}, ψ_{Ga}, w_{Te} and χ_{Te} are the amplitudes and phases of Ga occupational modulation and Te displacive modulation, respectively. We take the transverse type Te modulation which has the polarization vector along the z-axis.

The structure factor is then expressed as

$$\begin{aligned}F(Q) &= \sum_n f_n \exp\Big\{-2\pi i(hx_n + ky_n + lz_n)\\ &= \sum_n \sum_{n'} \sum_{n''} f_{Ga}[1 + \eta_{Ga}\sin\{2\pi(q_x na + q_y n'b) + \psi_{Ga}\}]\\ &\quad \times \exp\{-2\pi i(hna + kn'b + ln''c)\}\\ &\quad + \alpha f_{Te}\exp\{-2\pi i(hna + kn'b + l[n''c\\ &\quad + w_{Te}\sin\{2\pi(q_x na + q_y n'b) + \chi_{Te}\}])\Big\}\end{aligned} \tag{A.3}$$

where n, n' and n'' are the site indices along the x, y and z directions, a, b and c are the lattice constants which are set all equal in the present case, and α is the phase factor

$$\exp\{-\pi i/2(h + k + l)\} = (-i)^{(h+k+l)} \tag{A.4}$$

By using the Fourier development,

$$\exp(iz\sin\theta) = \sum J_m(z)\exp(im\theta) \tag{A.5}$$

where $J_m(z)$ is the Bessel function of the m-th order, we obtain the following expression for the satellite reflection

$$\begin{aligned}F(Q) &= +\frac{1}{2i}\sum_n \sum_{n'} \sum_{n''} \sum_m f_{Ga}\eta_{Ga}\exp(i\psi_{Ga})\\ &\quad \times \exp[-2\pi i\{(h - q_x)na + (k - q_y)n'b + ln''c\}]\\ &\quad - \frac{1}{2i}\sum_n \sum_{n'} \sum_{n''} \sum_m f_{Ga}\eta_{Ga}\exp(-i\psi_{Ga})\\ &\quad \times \exp[-2\pi i\{(h + q_x)na + (k + q_y)n'b + ln''c\}]\\ &\quad \sum_n \sum_{n'} \sum_{n''} \sum_m f_{Te}J_m(-2\pi l w_{Te})\exp(im\chi_{Te})\\ &\quad \times \exp[-2\pi i\{(h - mq_x)na + (k - mq_y)n'b + ln''c\}(-i)^{(h+k+l)}\end{aligned} \tag{A.6}$$

The summation over the site indices n, n' and n'' gives non-zero values only if, $2\pi(h - mq_x)a$, $2\pi(k - mq_y)b$ and $2\pi lc$ are multiples of 2π. The structure factor of the first order satellite reflection is given as,

$$\begin{aligned}F(Q) &= F(h \pm q_x, k \pm q_y, l) \propto \mp if_{Ga}\frac{\eta_{Ga}}{2}\exp(\pm i\psi_{Ga})\\ &\quad \mp (-i)^{(h+k+l)}f_{Te}J_1(2\pi l w_{Te})\exp(\pm i\chi_{Te})\end{aligned} \tag{A.7}$$

where we used the relation $J_{-m}(z) = (-1)^m J_m(z)$.

If we assume that the magnitude of the amplitude modulation of Ga atoms and that of the displacive modulation of Te atoms satisfy the condition $f_{Ga}\frac{\eta_{Ga}}{2} \approx f_{Te}J_1(2\pi lw_{Te})$, and also that the modulations are in phase ($\psi_{Ga} = \chi_{Te}$), Eq. (A.7) reproduces the observed pseudo extinction rule, i.e., if the main reflection has odd indices with $h+k+l = 4n+1$ the first order satellite reflection disappears, but, if $h+k+l = 4n-1$ the satellite reflection appears. The diffraction data also show that, for the satellite reflections with $q \approx 1/20[2\bar{1}0]_c$ the reverse is true.

References

[1] H. Hahn, W. Klinger, Z. Anorg. Chem. 259 (1949) 135–142.
[2] P.C. Newman, J.A. Cundall, Nature 200 (1963) 876.
[3] D. Luebbers, V. Leute, J. Solid State Chem. 43 (1982) 339–345.
[4] T. Hanada, Y. Nakamura, O. Nittono, Netsusyori 39 (1999) 57–58 (in Japanese).
[5] L. Kienle, V. Duppel, A. Simon, H.J. Deiseroth, Z. Anorg. Allg. Chem. 629 (2003) 1412–1420.
[6] Y. Otaki, Y. Yanadori, Y. Seki, K. Yamamot, S. Kashida, Acta Mater. 57 (2009) 1392–1398.
[7] A. Janner, T. Janssen, P.M. de Wolff, Acta Crystallogr. A 39 (1983) 658–666.
[8] C.D. Watkins, in: F.A. Funtley (Ed.), Lattice Defects in Semiconductors—1974, Institute of Physics, London, 1975, p. 1.
[9] R. Englman, The Jahn–Teller Effect in Molecules and Crystals, Wiley-Interscience, New York, 1972, p. 224.
[10] J.E. Bernard, A. Zunger, Phys. Rev. B 37 (1988) 6835–6856.
[11] A.G. Khachaturyan, Theory of Structural Transformations in Solids, Wiley, New York, 1983.
[12] J.W. Cahn, Acta Met. 10 (1962) 179–183.
[13] A. Guinier, X-ray Diffraction in Crystals, Imperfect Crystals, and Amorphous Bodies, Dover Publications, New York, 1994.
[14] Th. Karakostas, N.F. Flevaris, N. Vlachavas, G.L. Bleris, N.A. Economou, Acta Crystallogr. A 34 (1978) 123–126.